Rotation of single bacterial cells relative to the optical axis using optical tweezers

G. Carmon[1,2] and M. Feingold[1,2,*]

[1]*Department of Physics, Ben Gurion University, Beer Sheva 84105, Israel*

[2]*The Ilse Katz Center for Nanotechnology, Ben Gurion University, Beer Sheva 84105, Israel*

**Corresponding author: mario@bgu.ac.il*

Received August 17, 2010; revised November 11, 2010; accepted November 14, 2010;
posted November 29, 2010 (Doc. ID 133526); published December 21, 2010

Using a single-beam, oscillating optical tweezers, we demonstrate trapping and rotation of rod-shaped bacterial cells with respect to the optical axis. The angle of rotation, θ, is determined by the amplitude of the oscillation. It is shown that θ can be measured from the longitudinal cell intensity profiles in the corresponding phase-contrast images. The technique allows viewing the cell from different perspectives and can provide a useful tool in fluorescence microscopy for the analysis of three-dimensional subcellular structures.

OCIS codes: 180.6900, 110.2960.

Optical tweezers were first introduced by Ashkin *et al.* [1]. Their setup consisted of a single laser beam focused via a high-NA objective. It was shown that, because of the large gradient in the electric field, dielectric beads are trapped in the vicinity of the focal point. Since 1986, a wide range of optical tweezer techniques have been developed and applied in biology, chemistry, and physics, e.g., to probe the behavior of single DNA [2] and protein molecules [3], manipulate single cells [4], and measure the viscoelastic properties of solutions at micrometer length scales [5].

One line of research in optical trapping has dealt with upgraded optical tweezer setups that both trap and rotate microparticles. This was first achieved using two independent trapping beams to hold an extended object simultaneously at both ends. Moving one beam along a circular path while the other one is fixed forces the trapped object to follow the rotation [4,6]. In other systems, angular momentum is transferred from the laser beam to the trapped particle. One approach involves using Laguerre–Gaussian (LG) helical beams [7–9]. Such modes have well-defined orbital angular momentum that, together with the spin, is conveyed to the particle via absorption. Since absorption has to be low enough not to upset the trapping and avoid overheating, in this setup, particles rotate with relatively low angular velocities. Alternatively, it was shown that circularly polarized Gaussian beams can be used to rotate birefringent particles up to frequencies slightly over 1 KHz [10–14]. A third category of spanning optical traps employs asymmetrically shaped laser beams to align asymmetric microparticles [15–17]. Then, rotation of the beam will also rotate the trapped particle. A somewhat related approach was used in [18], where rotorlike microfabricated particles were shown to rotate in a regular Gaussian beam optical trap. Here, the linear momentum of the beam was converted to angular momentum of the particle.

All the techniques described in the previous paragraph rotate the trapped objects around the optical axis. They were motivated by the need to drive micromotors, to align micromachined components, or to mix in microfluidic devices. On the other hand, rotation of a trapped object may also be useful in the context of single cell microscopy. The ability to rotate a single cell with respect to the optical axis would allow imaging three-dimensional (3D) subcellular structures from different viewpoints. Scanning the angle between the long cell axis and the optical axis, θ, may allow reconstruction of the 3D structures using standard computerized tomography (CT) methods. Presently, the only setup that allows the scanning of θ consists of two or more optical traps that can hold an object at several different points [19,20]. Varying the relative heights of the traps leads to the desired rotation. Since there is a limit on the minimal distance between two optical traps, $d_{\min}$, this approach is restricted to large enough objects. Note that $d_{\min}$ is significantly larger along the optical axis than perpendicular to it. The smallest objects rotated relative to the optical axis using two traps were fused pairs of 2 μm diameter beads [20]. This was achieved with LG traps that are narrower along the optical axis than Gaussian traps.

In this Letter, we introduce a single-Gaussian-beam, optical tweezer method that allows scanning of θ. Its most straightforward implementation is for symmetric elongated objects, e.g., rod-shaped bacterial cells. It consists of a linear trap resulting from rapidly oscillating a standard Gaussian trap by means of a galvanometric mirror (Fig. 1). Raising the amplitude of the oscillation, A, from 0 to the length of the object, L, corresponds to varying θ from 0°, vertical orientation, to 90°, horizontal orientation (Fig. 2). This behavior interpolates between two well-known extreme cases: 1. vertical alignment of elongated objects in standard traps, and

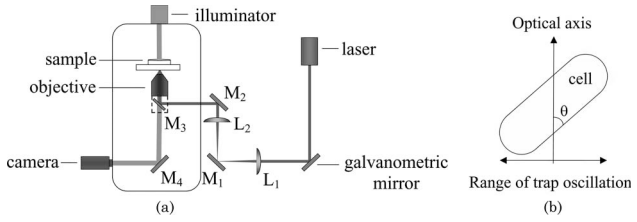

Fig. 1. (a) Experimental setup: M_1 to M_4, mirrors (M_3 is a dichroic mirror); L_1, L_2, lenses (telescope). (b) Schematic view of a rotated cell.

2. horizontal alignment of elongated objects in linear traps longer than L. Our θ scanning approach is significantly simpler than that of multiple traps. In particular, it can rotate bacterial cells that are about the same size as the fused beads of [18] without the need of higher-order beams.

The optical system consists of an IX70 inverted Olympus microscope with an UPLFLN 100XO2PH, 1.3 NA oil immersion objective used for both imaging and the optical trap (Fig. 1). A single galvanometric mirror is located along the optical path of the laser beam (SDL, $\lambda = 830$ nm) and is driven by a function generator. Lenses L_1 and L_2 conjugate the plane of the galvanometric mirror to the back aperture of the objective. In this configuration, tilting the galvanometric mirror rotates the laser beam around its axis at the entrance aperture of the objective [21]. Thus, the trap structure is preserved while the beam scans the image plane. The objective back aperture is 7 mm wide, truncating the Gaussian beam at 2.7σ. Oscillating the galvanometric mirror at 100 Hz effectively generates a steady, horizontal, linear trap. Its length is determined by the amplitude of the oscillation. A sinusoidal wave was used to scan the galvanometric mirror. There was no observable difference in the rotation of elongated objects when using other wave forms, e.g., sawtooth.

We have tested our setup using fixed *E. coli* cells grown in Lurie Broth medium until the optical density at 600 nm reached about 0.2, which is in the exponential growth regime. For simplicity, we only study cells that have not yet started to divide. Their shape is almost exactly that of a cylinder with hemispherical caps [22] and their size is about 1 μm $\times$ 3 μm. Because *E. coli* have a highly rigid cell wall, their shape is not affected by the trapping forces [23]. In Fig. 2, we show a θ scan with a 15° step for a typical *E. coli* cell obtained by varying A from 0 to L, but much finer θ scans can also be performed.

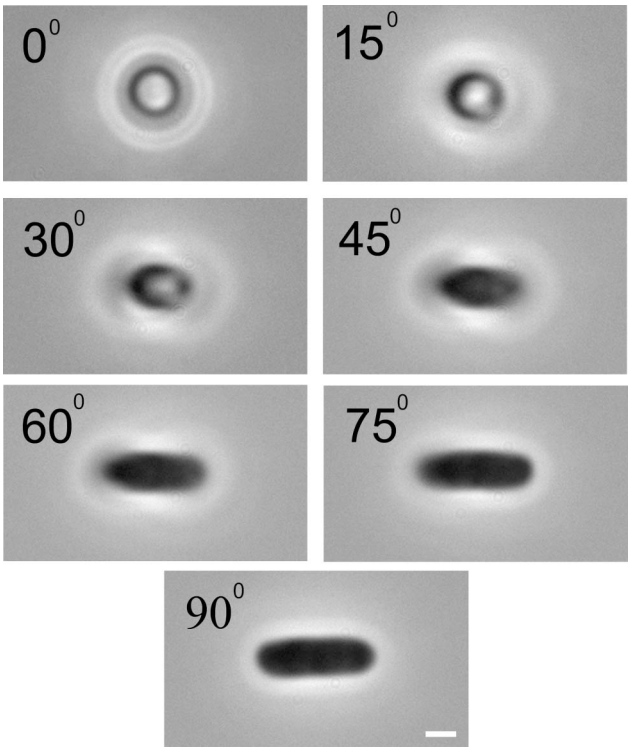

Fig. 2. A large step θ scan of an *E. coli* cell. Angles 30°, 45°, 60°, 75°, and 90° were measured using the critical point method, 15° is obtained via the interpolation approach, and 0° corresponds to the case of a nonoscillating trap. Bar = 1 μm.

Although phase-contrast imaging cannot reveal the internal structure of the cells, it can be used to measure the orientation angle, θ. However, since the cell caps become strongly defocused at even small deviations from the horizontal orientation, this becomes a challenging task. To overcome this difficulty and measure θ, we use a height library of horizontally oriented defocused cell images. First, the same cell as in the θ scan is horizontally aligned. Then, we gradually vary the height of the trap by means of small, stepwise changes in the distance between the telescope lenses, L_1 and L_2 Fig. 1. This allows scanning the trap height over a range of about 1.5 μm on each side of the focal plane. Our height library consists of the recorded cell images at each step of the height scan. Although the images in the library are quite different from each other, we find that, within experimental error, all the longitudinal intensity profiles intersect at two locations, one near each of the cell ends. We refer to these locations as critical points. This behavior is reminiscent of the focus invariant intensity points in the bright-field image of a straight edge [24,25]. The distance between the critical points, L_{cp}, provides an approximation to the cell length, L. Within a few micrometers of the focal plane, L_{cp} is invariant under defocusing translations, and so is the value of the phase contrast intensity at the critical points, I_{cp}. Our main assumption is that I_{cp} is not affected by rotation. In other words, in the rotated cell, each of the defocused cell caps will have its own critical point located where its longitudinal intensity profile equals I_{cp}. As in the horizontal orientation, these critical points lie in the vicinity of the cell edge. It follows that the distance between the critical points of the rotated cell corresponds to the projected L_{cp} on the imaging plane, $L_{\mathrm{cp}} \sin\theta$, allowing us to deduce θ.

The critical point approach fails at angles that are less than about 25° where, in the image, the cylindrical section of the cell largely overlaps with its caps (Fig. 2). Instead, to estimate the value of θ in the $(0°, 25°)$ range, we measure the deviation of the cell image from circular symmetry. Such deviation may be quantified by the ratio between the length and the width, $R_{\mathrm{LW}}(\theta)$, of a cell contour corresponding to an intensity that is slightly below the background level. Because $R_{\mathrm{LW}}(0°) = 1$ and $R_{\mathrm{LW}}(30°) = 1.54$, this allows us to approximate θ by linearly interpolating $R_{\mathrm{LW}}(\theta)$ over the $(0°, 30°)$ range.

We have tested the critical point method using cells that were immobilized by attaching one of their caps to the glass bottom of the sample. The optical trap allows immobilizing the *E. coli* at different orientations (different θ). For such cells, and when $\theta > 25°$, we can focus separately on each of the cell caps and obtain the corresponding position of the cell edge [26]. This allows us to determine θ from the geometry of the problem, θ_g. We have compared these values of θ with those obtained by the critical point method, θ_{cp} (Fig. 3) and found that $\theta_g \cong \theta_{\mathrm{cp}}$ within experimental error. The geometric measurement of θ for immobilized cells fails in the small θ range, $\theta < 25°$, for the same reason that prevented the

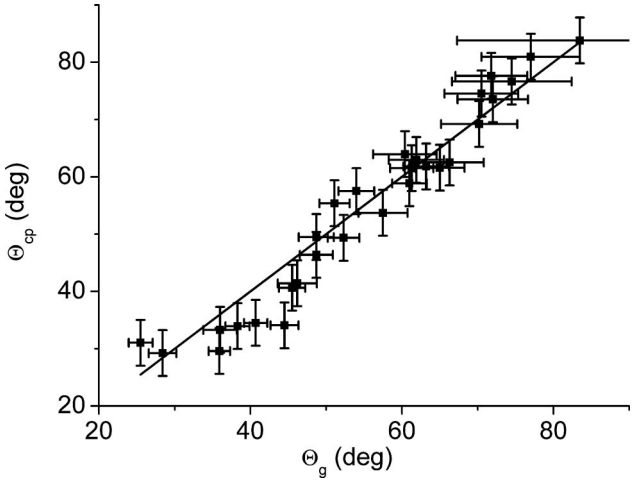

Fig. 3. Testing the critical point method. For *E. coli* cells that were attached to the glass bottom of the sample in different orientations, we compare θ_{cp} with θ_g (squares). The $\theta_g = \theta_{cp}$ line is also shown.

use of the critical point method in this range. That is, for $\theta < 25°$, the longitudinal cell edge can no longer be reliably distinguished from the vertical cell edge. As a result, we could not test the accuracy of the θ values obtained using our interpolation approach.

In conclusion, we have introduced a technique that allows rotating and aligning elongated micro-objects around an axis normal to the laser beam. Its implementation is simpler than the competing multiple-trap approach, as it requires only adding a galvanometric mirror to a standard optical tweezer system. We suggest that this method may become a useful tool in cellular imaging, because it can provide different viewpoints on 3D subcellular structures. In particular, it could be used for the realization of single-cell CT imaging.

We thank I. Abdulhalim, A. Braiman, and I. Fishov for useful discussions. This research was supported in part by the Israel Academy of Science and Humanities (grant no. 1544/08).

References

1. A. Ashkin, J. M. Dziedzic, J. E. Bjorkholm, and S. Chu, Opt. Lett. **11**, 288 (1986).
2. S. R. Quake, H. Babcock, and S. Chu, Nature **388**, 151 (1997).
3. D. A. Schafer, J. Gelles, M. P. Sheetz, and R. Landick, Nature **352**, 444 (1991).
4. A. Ashkin, J. M. Dziedzic, and T. Yamane, Nature **330**, 769 (1987).
5. D. Velegol and F. Lanni, Biophys. J. **81**, 1786 (2001).
6. H. Misawa, K. Sasaki, M. Koshioka, N. Kitamura, and H. Masuhara, Appl. Phys. Lett. **60**, 310 (1992).
7. H. He, M. E. J. Friese, N. R. Heckenberg, and H. Rubinsztein-Dunlop, Phys. Rev. Lett. **75**, 826 (1995).
8. M. E. J. Friese, J. Enger, H. Rubinsztein-Dunlop, and N. R. Heckenberg, Phys. Rev. A **54**, 1593 (1996).
9. N. B. Simpson, K. Dholakia, L. Allen, and M. J. Padgett, Opt. Lett. **22**, 52 (1997).
10. E. Higurashi, R. Sawada, and T. Ito, Appl. Phys. Lett. **73**, 3034 (1998).
11. M. E. J. Friese, T. A. Neiminen, N. R. Heckenberg, and H. Rubinsztein-Dunlop, Nature **394**, 348 (1998).
12. S. Juodkazis, M. Shikata, T. Takahashi, S. Matsuo, and H. Misawa, Appl. Phys. Lett. **74**, 3627 (1999).
13. E. Higurashi, R. Sawada, and T. Ito, Phys. Rev. E **59**, 3676 (1999).
14. E. Higurashi, R. Sawada, and T. Ito, J. Micromech. Microeng. **11**, 140 (2001).
15. S. Sato, M. Ishigure, and H. Inaba, Electron. Lett. **27**, 1831 (1991).
16. L. Paterson, M. P. MacDonald, J. Arlt, W. Sibbett, P. E. Bryant, and K. Dholakia, Science **292**, 912 (2001).
17. A. T. O'Neil and M. J. Padgett, Opt. Lett. **27**, 743 (2002).
18. E. Higurashi, H. Ukita, H. Tanaka, and O. Ohguchi, Appl. Phys. Lett. **64**, 2209 (1994).
19. K. Visscher, G. J. Brakenhoff, and J. J. Krol, Cytometry **14**, 105 (1993).
20. V. Bingelyte, J. Leach, J. Courtial, and M. J. Padgett, Appl. Phys. Lett. **82**, 829 (2003).
21. E. Fällman and O. Axner, Appl. Opt. **36**, 2107 (1997).
22. E. Itan, G. Carmon, A. Rabinovitch, I. Fishov, and M. Feingold, Phys. Rev. E **77**, 061902 (2008).
23. X. Yao, M. Jericho, D. Pink, and T. Beveridge, J. Bacteriol. **181**, 6865 (1999).
24. A. Glindemann and J. Kross, J. Mod. Opt. **38**, 379 (1991).
25. M. Gu and C. J. R. Sheppard, Appl. Opt. **33**, 625 (1994).
26. G. Reshes, S. Vanounou, I. Fishov, and M. Feingold, Biophys. J. **94**, 251 (2008).